

*Ідентифіковано параметри інвертора напруги тягового приводу на базі синхронного двигуна зі збудженням від постійних магнітів. Синтезовано імітаційну модель тягового приводу, що дозволяє отримати миттєві значення електричних втрат в інверторі та двигуні. Проаналізовано залежність електричних витрат від швидкості руху поїзда та тактової частоти інвертора*

*Ключові слова: тяговий синхронний двигун зі збудженням від постійних магнітів, електричні втрати*

*Идентифицированы параметры инвертора напряжения тягового привода на базе синхронного двигателя с возбуждением от постоянных магнитов. Синтезирована имитационная модель тягового привода, позволяющая получить мгновенные значения электрических потерь в инверторе и двигателе. Проанализирована зависимость электрических потерь от скорости движения поезда и тактовой частоты инвертора*

*Ключевые слова: тяговый синхронный двигатель с возбуждением от постоянных магнитов, электрические потери*

# DETERMINING ELECTRICAL LOSSES OF THE TRACTION DRIVE OF ELECTRIC TRAIN BASED ON A SYNCHRONOUS MOTOR WITH EXCITATION FROM PERMANENT MAGNETS

**B. Liubarskyi**

Doctor of Technical Sciences, Professor\*

E-mail: lboris1911@ukr.net

**O. Demydov**

Senior Lecturer\*

E-mail: pz100500@ukr.net

**B. Yeritsyan**

PhD\*

E-mail: bagish\_ericjan@ukr.net

**R. Nuriiev**

Postgraduate student\*

E-mail: ramkhua@gmail.com

**D. Iakunin**

PhD, Associate Professor\*

E-mail: Unicomber@ukr.net

\*Department of Electrical transport and diesel locomotives construction

National Technical University «Kharkiv Polytechnic Institute»  
Kyrpychova str., 2, Kharkiv, Ukraine, 61002

## 1. Introduction

Modern trends in the development of electric rolling stock necessitate the creation of advanced energy-saving technologies for a traction electric drive [1]. One of the ways to improve energy efficiency is to decrease energy costs in the operation of a traction drive [2–4]. The other way is to create traction drives based on the new, promising types of electromechanical energy converters, traction engines, such as induction [2–4], reactive inductor [5], and synchronous motors with excitation from permanent magnets [6] (SMPM). The latter possess high energy indicators as a result of the absence of losses for excitation [1]. To determine the optimal operational modes of SMPM, the procedures are required that would make it possible to identify losses and components under all operational modes of the traction drive.

Losses in the traction drive are composed of 3 main parts: losses in a traction motor, losses in a converter, and losses in mechanical part of the drive. A procedure for determining losses in a traction motor is described in [7], losses in a traction converter are determined by the procedure given in [8–10]. Losses in mechanical part are calculated according to the procedure described in [11].

However, the above scientific literature [7–11] outlines procedures for calculation losses in the elements of the traction drive, but not comprehensively in the traction drive in general. The procedure given in [10] employs the averaged calculation of current parameters of electronic keys. This does not make it possible to vary certain parameters of the converter and the motor and to determine their influence on the combined performance efficiency coefficient of the drive, which makes it impossible to solve an optimization problem using the criterion of maximum performance efficiency coefficient of the drive in general.

Therefore, the study that aims to construct a procedure for determining total losses of the drive in general, appears relevant.

## 2. Literature review and problem statement

Reducing energy expenditure in the operation of a traction drive can be achieved by using new types of engines [5, 6], inverter topologies [12], control systems [13], as well as by improving characteristics of existing systems, which is attained by various means. To assess the energy efficiency of

the drive, it is convenient to use the magnitudes of losses in its elements – the traction motor and the inverter.

Papers [13–17] address the issue on determining losses in the engine. Authors of [13], based on the modeling of SMPM, compiled a table of losses in a traction engine, using which makes it possible to create a control system optimized for the engine’s performance efficiency coefficient. Paper [14] proposed a model of losses in SMPM, taking into account losses in steel and copper; and reported a procedure, which makes it possible to determine with high accuracy the harmonic composition of the phase current. [15] describes a procedure for choosing the optimal clock frequency of the inverter and the engine’s control angle in the composition of a direct traction drive in a vehicle. Authors of [16] proposed the algorithm of synchronous PWM, which ensures an improved harmonic composition of stator currents in a wide range of modulation coefficients and control angles at relatively low clock frequency of the inverter. [17] applied a dynamic model of SMPM that accounts for losses in steel and proposed an algorithm to control a drive based on SMPM, which makes it possible to reduce losses in engine without significantly compromising the dynamic qualities of the drive in general.

Paper [18] that addresses determining losses in the inverter’s transistors considered losses in conductivity, turning on and off; the authors performed linearization and derived analytical expressions for the dynamic losses in transistors; they, however, did not consider losses for the antiparallel diode reverse recovery.

Authors of the above studies determine losses either in the inverter or in a traction engine. They failed to consider that improving energy efficiency parameters in one of the links, which includes a drive (an inverter, an engine), can degrade parameters in another link. Traction drive is an integrated device; end user is interested in its energy efficiency in general; it is desirable to provide for the determining of losses in the inverter and in the engine in their joint work so that their mutual influence is taken into consideration.

Papers [19, 20] determine losses in the inverter and in the engine comprehensively. Author of [19] proposed analytical formulae for determining losses in the engine from the main frequency and higher harmonics of phase current, as well as losses in the inverter’s transistors. In [20], losses in the inverter are determined using a simulation of the inverter, while losses in the traction motor are calculated by the finite element method. Optimum clock frequency of the inverter was also chosen based on the drive’s performance efficiency coefficient.

The shortcoming of procedures given [19, 20] is the calculation of losses in transistor using averaged formulae that do not make it possible to take into account the dependence of energy of enabling and disabling the transistors, energy of the antiparallel diode reverse recovery, and other reference characteristics of transistors, on the current that passes through them.

There is a separate task on determining parameters of cooling systems in the components of the traction drive – inverter and motor.

In [21], author proposed a procedure for determining parameters of the cooling system of SMPM; the degree of engine heating is determined based on the magnitudes of electrical losses in it. Authors of [22], based on the iterative electrical and thermal simulation of power transistors of the inverter, obtained data for designing a cooling system of the inverter. When applied in tandem, these procedures make it possible to calculate the cooling system of the drive in general.

The analysis of the scientific literature revealed that none of the procedures suggested above makes it possible to fully determine losses in all links of the electric drive taking into consideration the dependence of parameters of power elements of the inverter on the instantaneous values of current that passes through them.

### 3. The aim and objectives of the study

The aim of present study is to develop a procedure for determining electric losses in the traction drive based on synchronous motors with excitation from permanent magnets. This would make it possible to identify the components of losses in the traction drive depending on the clock frequency of PWM.

To accomplish the aim, the following tasks have been set:

- to build a simulation model of the traction drive that makes it possible to calculate the instantaneous values of losses in the traction inverter;
- to devise a procedure that would make it possible to calculate losses in the traction motor depending on the obtained current form of the phase current.

### 4. Simulation model of the traction drive, which makes it possible to obtain instantaneous values of losses in the traction inverter

To determine losses in a reducer-free traction drive of the electrical train with a capacity of 80 kW and a maximum rotation frequency of 320 rpm, we have devised a procedure, which was implemented using a digital simulation of the drive in the programming environment Matlab-Simulink [23]. Its general block diagram is shown in Fig. 1.

Subsystem AIN is the bridge three-phase voltage inverter based on IGBT transistors.

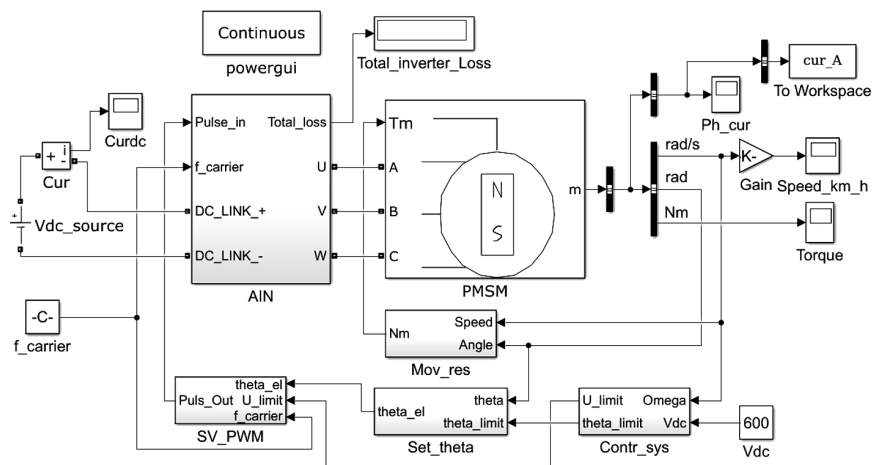


Fig. 1. General block diagram of digital simulation of the drive

Unit Permanent Magnet Synchronous Machine is a synchronous motor with excitation from permanent magnets with a measuring unit.

Subsystem Move\_res calculates equivalent resistance of the electrical train motion in accordance with [24].

Subsystem Contr\_sys together with subsystem Set\_theta assign the phase voltage and switching angle depending on the rotation frequency. This enables a transition between zones of current limit, power, and weakening of the field.

Subsystem SM\_PWM executes algorithm of space-vector modulation of transistors in the voltage inverter.

Fig. 2 shows the Contr\_sys subsystem.

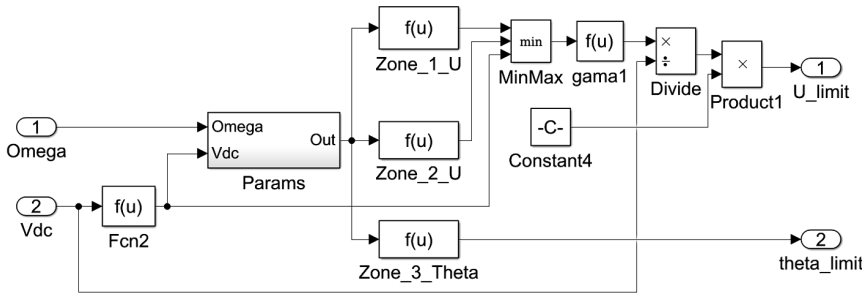


Fig. 2. Design of subsystem Contr\_sys

The subsystem generates signals to control the magnitude of phase voltage and a signal to assign control angle.

The system consists of three independent channels Zone\_1\_U, Zone\_2\_U, and Zona\_3\_Theta.

Unit Zone\_1\_U is intended to compute the magnitude of assigning the voltage of the engine under the current limit mode.

Unit Zone\_2\_U is intended to calculate the magnitude of setting the voltage of the engine under a permanent power mode.

Unit Zone\_3\_Theta is intended to compute the magnitude of assigning the angle of inverter's switching under a mode of the engine's weakened field.

The unit of constants Params is intended for setting the engine's parameters.

Subsystem PV\_SVM, shown in Fig. 3, executes the algorithm of space-vector modulation of keys for the voltage inverter according to the algorithms described in [25, 26].

The clock frequency of space-vector PWM is assigned from the outside, using the constant f\_carrier. The clock frequency signal arrives at the input to subsystem SV PWM; along with a voltage limitation signal U\_limit, it defines parameters of the sawtooth reference signal SAW.

The subsystem also receives a signal of absolute encoder theta\_el. Units To\_360\_deg and To\_60\_deg isolate from the encoder's signal periodic sequences JBIG at 360 and 60 degrees, which correspond to a spatial vector performing a full rotation and passing a sector, respectively.

Units Set\_K1 and Set\_K2 calculate coefficients of filling separate phases according to the current position of a spatial vector in a given sector.

Units A\_pulse, B\_pulse convert coefficients of filling separate phases into switching pulses to generate a spatial vector for the same sector. Allocation of switching pulses between all sectors is assigned to unit Set\_sector, which defines a sector for the spatial voltage vector, and allocating subsystem Commutator\_deltic.

Subsystem AIN consists of six identical units of electronic key g1...g6. Every electronic key consists of units that implement an IGBT-transistor, a reverse diode, and a snubber. A built-in gauge defines voltage in transition collector-emitter and current through the transistor and diode. Controlling pulses to open transistors are transmitted using terminal In1, which contains 6 signals simultaneously.

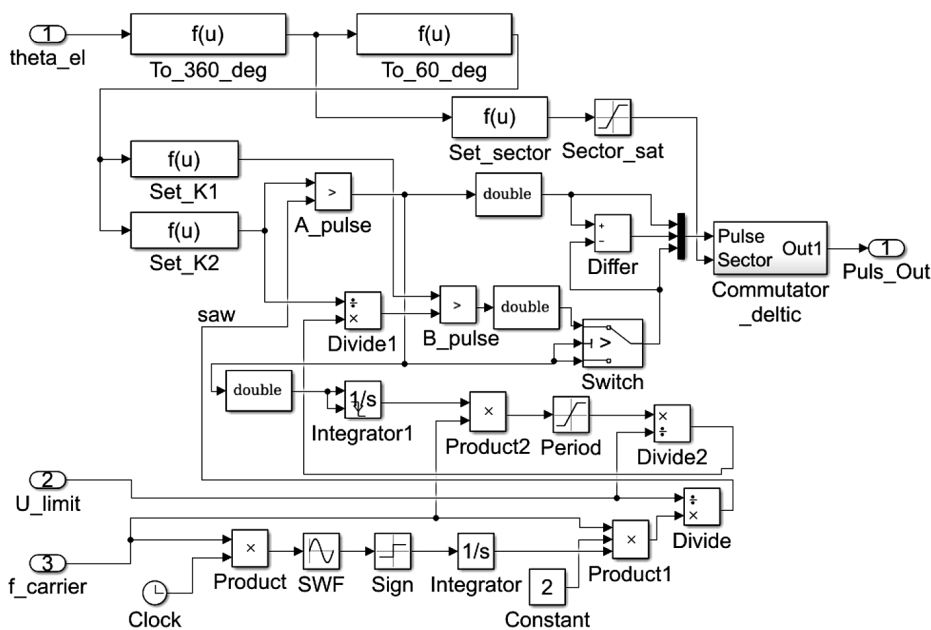


Fig. 3. Design of subsystem SV\_PWM

A DC link is connected to AIH through terminals DC\_LINK\_ and DC\_LINK\_+; the engine is connected through terminals U, V, W.

The calculation of electrical losses in the inverter is assigned to identical subsystems HI\_losses and LO\_losses that compute losses in the upper and lower IGBT-transistors of the transistor rack, as well as losses in the reverse diodes and snubbers. The total losses are added and multiplied by 3.

Loss counters in the inverter are shown in Fig. 5; they define the magnitudes of the following components: losses of conductivity in the antiparallel diode and IGBT transistor, switching losses in the IGBT transistor, losses in the antiparallel diode reverse recovery, and losses in a snubber's resistor. Simulation of the drive operation is executed in time intervals of 1 second, thus the total energy, accumulated during simulation, is equal to the power of losses.

Losses in the inverter are determined similar to the procedure given in [8, 10]. The main difference of the proposed procedure is the direct calculation of parameters of the electronic key according to the instantaneous value of current, that passes through them, and reference data [27].

Losses of conductivity in the antiparallel diode are calculated in the subsystem DIODE\_CONDUCTION\_LOSSES, which is shown in Fig. 6. Direct voltage drop on a diode diod\_conductivity\_U is determined according to the module of existing current and the dependence given in a reference book. Element Diod\_current selects a negative current through the power device that corresponds to the current passing through an antiparallel diode. Units Zero-Order Hold and Integrator1 integrate the resulting value of losses throughout the time of simulation.

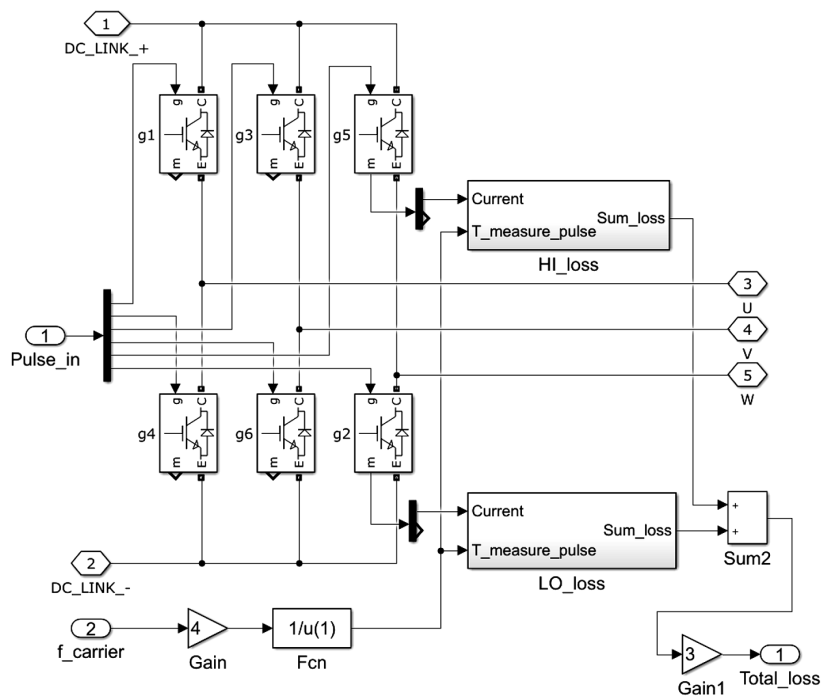


Fig. 4. Design of subsystem AIN

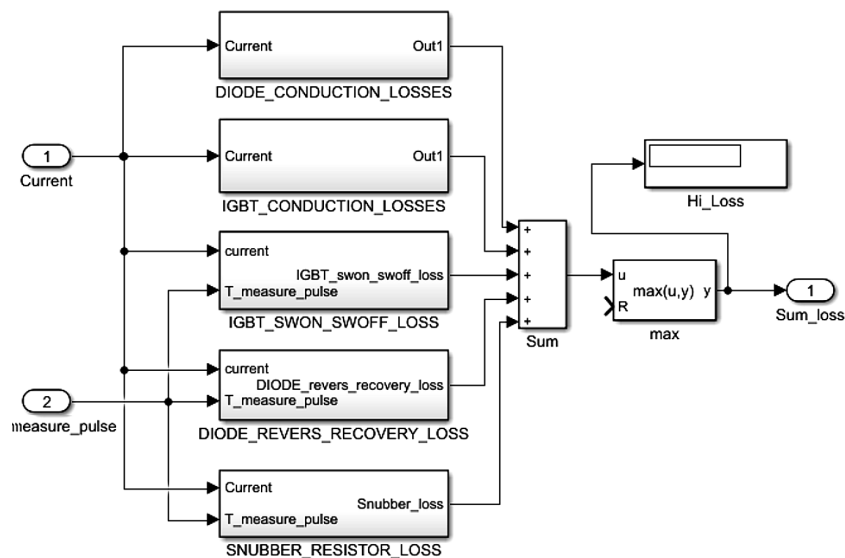


Fig. 5. Counter of losses in the inverter

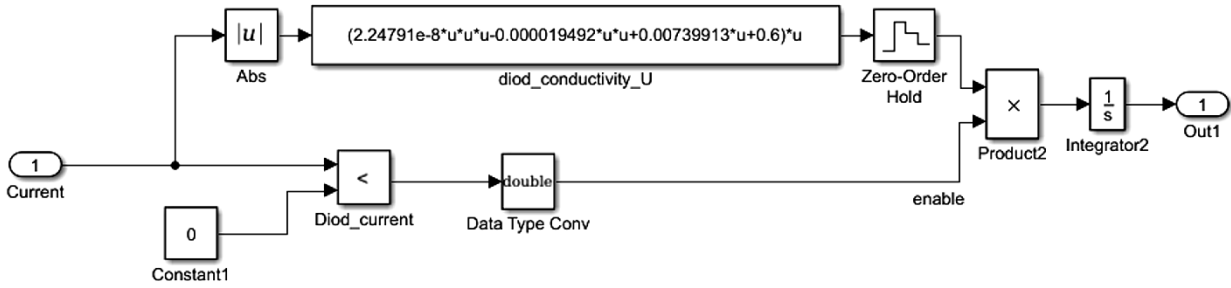


Fig. 6. Subsystem DIODE\_CONDUCTION\_LOSSES

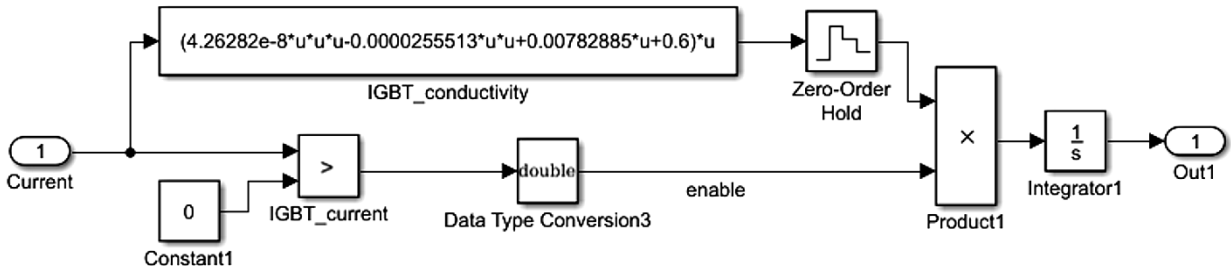


Fig. 7. Subsystem IGBT\_CONDUCTION\_LOSSES

Subsystem IGBT\_CONDUCTION\_LOSSES, shown in Fig. 7, calculates losses in the conductivity of IGBT-transistors and operates similarly to the above subsystem DIODE\_CONDUCTION\_LOSSES. Element IGBT\_current selects positive current through a power device that makes it possible to accumulate the energy of losses in the integrator.

Subsystem IGBT SWON SWOFF LOSSES is designed to calculate losses for enabling and disabling the IGBT transistor; it is shown in Fig. 8. Unit Compare1 selects positive pulses of current through a power device, thereby cutting off the pulses of current through the antiparallel diode. Units Hit Crossing and Hit Crossing1 emit signals for the moment of enabling and disabling the IGBT transistor, respectively. Signals from these units are delivered to subsystems Current\_fixer\_swon and Current\_fixer\_swoff. These subsystems register the value of current that passes through the IGBT transistor at the moments of enabling and disabling. A signal from unit Hit Crossing is also sent to the J-K trigger whose outputs state changed to the opposite every time the

transistor is turned on. By using units Variable Transport Delay, Variable Transport Delay1, logical units, and signal T\_measure\_pulse, we isolate signals with a length of of the clock frequency cycle at moments the transistors are turned on. The signals received are merged using logical operator OR and are multiplied by the magnitude inverse to of the clock frequency cycle of the inverter. Thus, we generate pulses of a single amplitude that arrive at the moments the transistor is enabled. Fixed values of current from subsystems of Current\_fixer\_swon and Current\_fixer\_swoff are passed to units Eswon, Eswoff, which calculate the energy for enabling and disabling the transistor according to reference data [27] and current at the moments of enabling and disabling, after which the obtained values are summed up.

By using units Prod3 and Int3 we obtain a uniformly ascending curve, which corresponds to the accumulated value of the energy for enabling and disabling. Energy, accumulated over 1 second of operation of the inverter, is equal to the power of losses for switching the IGBT transistor.

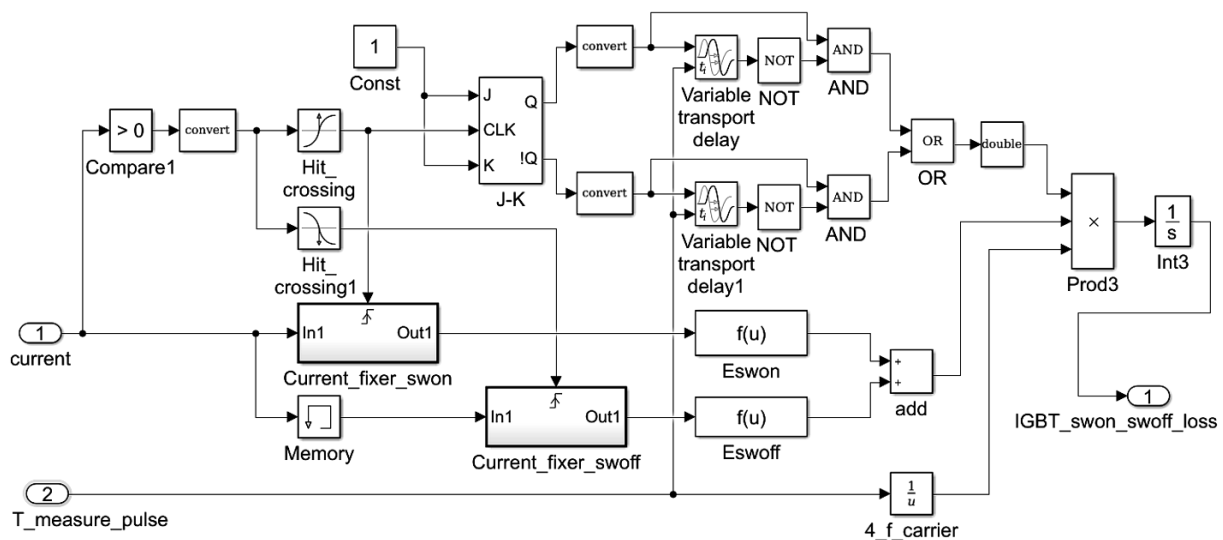


Fig. 8. Subsystem IGBT\_SWON\_SWOFF\_LOSSES

Subsystem DIODE\_REVERS\_RECOVERY\_LOSSES is shown in Fig. 9 and intended to calculate losses for the antiparallel diode reverse recovery. Unit Compare1 selects negative pulses of current through a power device, thereby cutting off the pulses of current through the IGBT transistor. Units Hi and Hit generate signals for the moment of enabling and disabling, respectively. A signal from unit Hit is sent to subsystem Current\_fixer. This subsystem registers the value of current that passes the antiparallel diode at the time of reverse recovery.

A signal from unit Hi is sent to the J-K trigger whose outputs state changed to the opposite every time the transistor is turned on. By using units Variable Transport Delay, Variable Transport Delay1, logical units, and signal T\_measure\_pulse, we isolate signals with a length of 1/4 of the clock frequency cycle at the moments of reverse recovery of the diode. The received signals are merged using the logical operator OR and are multiplied by the magnitude inverse to 1/4 clock frequency cycle of the inverter. Thus, we generate pulses of a single amplitude that arrive at the moments of antiparallel diode reverse recovery.

A fixed value of current from subsystem Current\_fixer is sent to unit Err, which calculates energy of the antiparallel diode reverse recovery according to the reference data from the IGBT transistor and current at the moments of reverse recovery.

By using units Product and Integrator, we obtain a uniformly ascending curve, which corresponds to the accumulated value of the energy of reverse recovery, Energy, accumulated over 1 second of operation of the inverter, is equal to the power of losses for the antiparallel diode reverse recovery.

Subsystem SNUBBER\_RESISTOR\_LOSSES is shown in Fig. 10 and is intended to determine the magnitude of energy dissipated in the snubber resistor. The traction inverter employs a fixing snubber RC-chain; connection circuit and the rated value of the snubber capacitor were selected in accordance with [9]. The value of inductance of a DC link, typical for voltage inverters with such capacity, is selected in accordance with [8]. Unit Comp cuts off the negative current pulses. Unit Hit Crossing selects moments for disabling the power transistor. A signal from unit Hit Crossing is sent to the J-K trigger whose outputs state changes to the opposite every time the transistor is turned off.

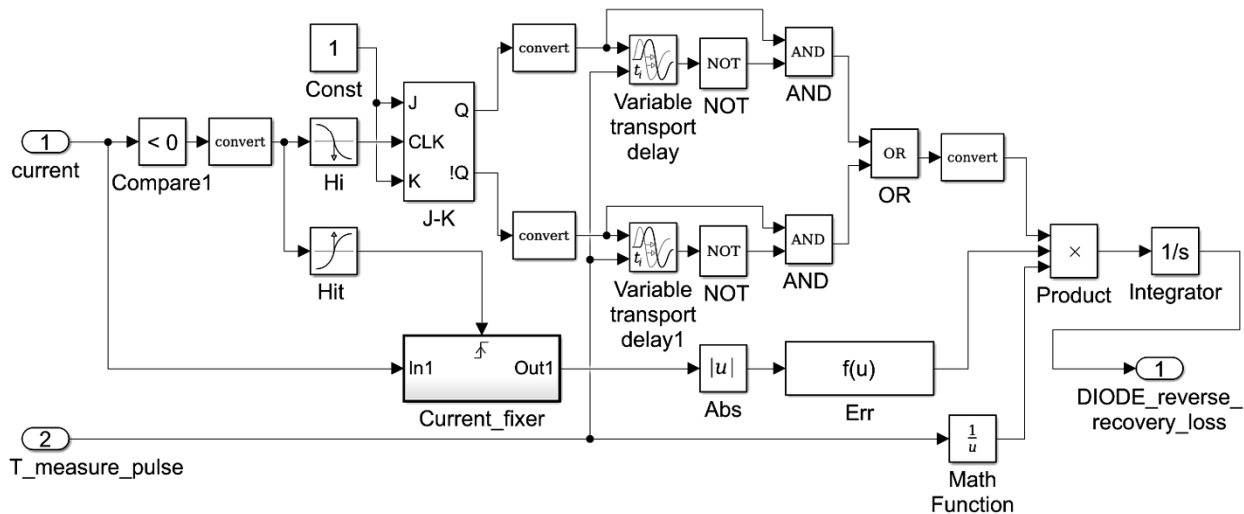


Fig. 9. Subsystem DIODE\_REVERS\_RECOVERY\_LOSSES

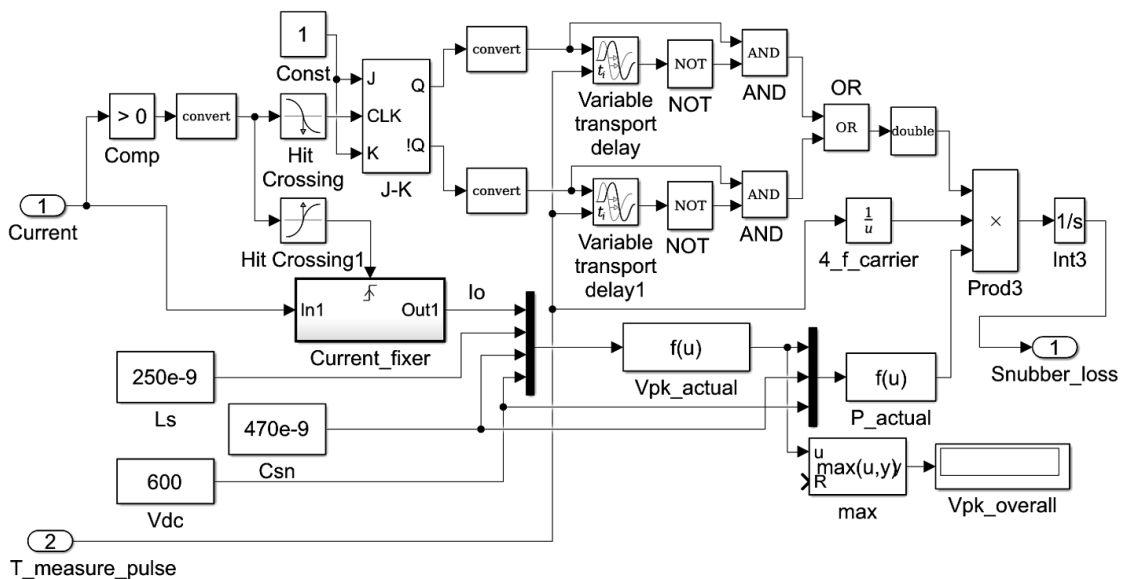


Fig. 10. Subsystem SNUBBER\_RESISTOR\_LOSSES

By using units Variable Transport Delay, Variable Transport Delay1, logical units, and signal T\_measure\_pulse, we select signals with a length of ¼ of the clock frequency cycle at the moments of disabling the IGBT-transistor, which corresponds to the moment of triggering a fixing snubber. The received signals are merged using the logical operator OR and are multiplied by the magnitude inverse to ¼ clock frequency cycle of the inverter. Thus, we receive pulses of a single amplitude that arrive at the moments of triggering a snubber.

A signal from unit Hit Crossing1 is sent to subsystem Current\_fixer. This subsystem registers the value of current that passes through the IGBT transistor at the moment it is turned on. Unit Vpk\_actual, by using the obtained value of current, as well as the assigned inductance, DC link voltage, and capacitance of the snubber capacitor, defines the magnitude of voltage release when disabling the IGBT transistor. The magnitude of voltage release determines the required class of power transistor.

By using units Prod3 and Int3, we obtain a uniformly ascending curve that corresponds to the accumulated value of energy, dispersed in a snubber's resistor. Energy, accumulated over 1 second of operation of the inverter, is equal to the power of losses in the snubber's resistor.

### 5. Determining losses in the traction engine

Losses in traction engine are divided into 2 groups – losses in steel and losses in copper. To calculate the magnitude of losses, one employs geometrical and electrical parameters of the traction engine, as well as the shape and amplitude value

of the phase current, obtained as a result of simulation of different modes of operation of the traction drive.

The result of modeling the operation of the traction drive is the constructed chart of phase currents, shown in Fig. 11. It clearly demonstrates a shape of the current close to the sinusoid at the main frequency of the inverter, as well as small fluctuations of current at the PWM clock frequency due to the pulse nature of work of the voltage inverter.

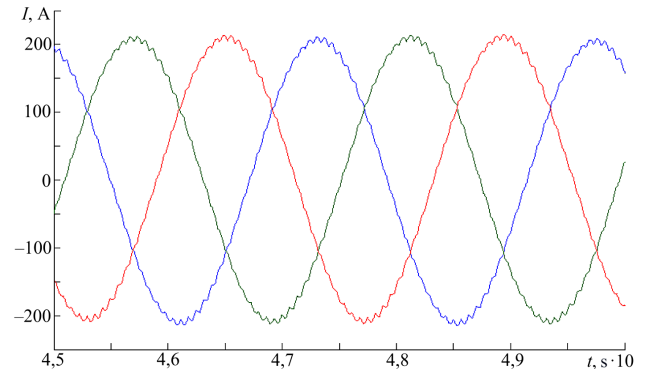


Fig. 11. Phase currents of traction engine

By using unit powergui, embedded in the software package Matlab-Simulink, we decompose current of the phase into a Fourier series. This is the technique to determine the amplitude of current at the main frequency of the inverter, which is directly involved in the creation of electromagnetic torque of the engine, as well as the frequency and amplitude of higher harmonic components of the phase current. Example of the phase current decomposition into a Fourier series is shown in Fig. 12.

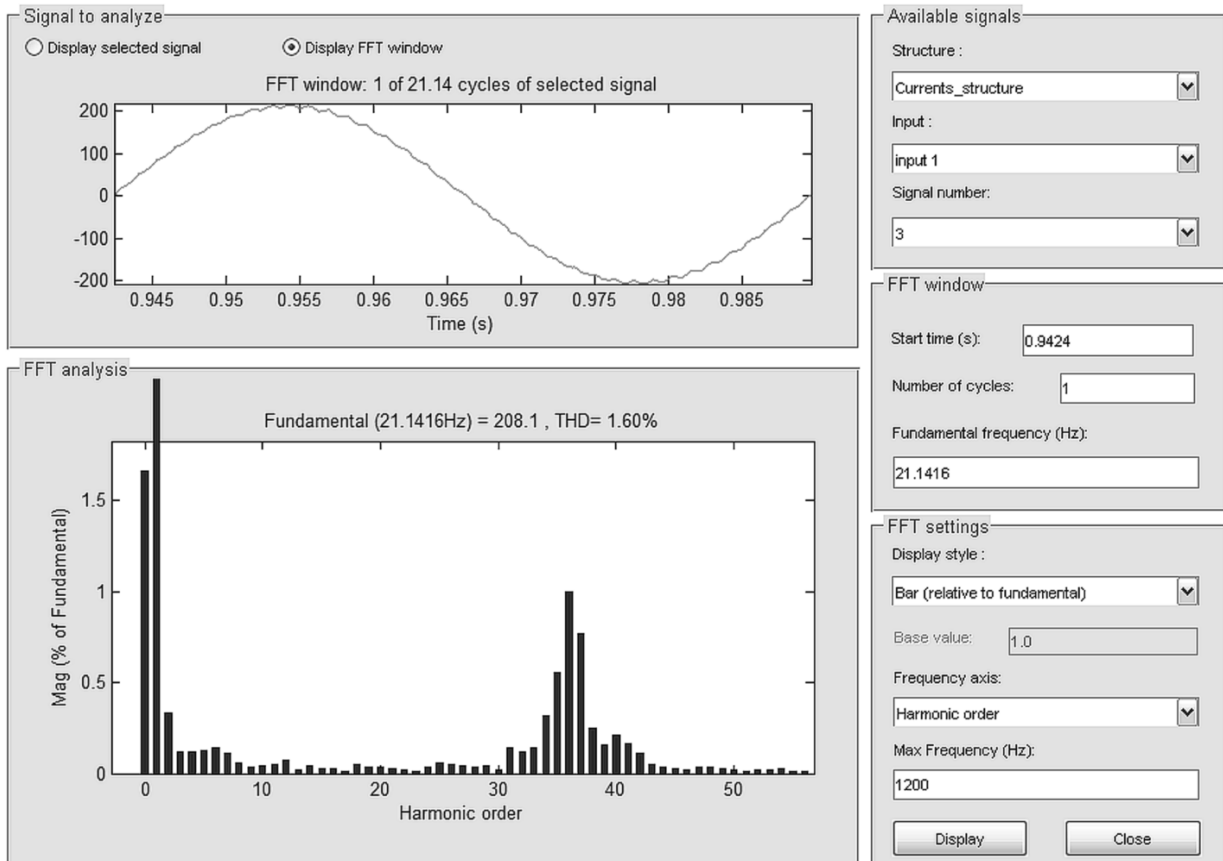


Fig. 12. Results of the engine's phase current decomposition into a Fourier series

The distribution histogram of amplitudes of higher harmonic components clearly demonstrates a column of the first harmonic, as well as a group of harmonics from 34 to 37, which correspond to oscillations at the PWM clock frequency. The latter allow us to assess the impact of the chosen value for clock frequency of the inverter on the losses within the engine.

Based on the data acquired, we determine losses in copper and in steel at the basic frequency, as well as at higher harmonics whose amplitude exceeds 0.3 % of the amplitude of the basic frequency. The sum of losses at the basic frequency and higher harmonics determines total losses.

Calculation of the magnitude of losses is carried out similar to the procedure described in [7]; the signature of the procedure is the application of the phase current decomposition, obtained as a result of imitation simulation of the traction drive. L

Losses in the steel of the engine's stator back are derived from the following formula:

$$P_a = 2,7 \cdot B_a^2 \cdot mag^2 \cdot m_a \left[ 0,044 \cdot f_n + 5,6 \cdot \left( \frac{f_n}{100} \right)^2 \right], \quad (1)$$

where  $B_a$  is the induction in the back of the stator,  $mag$  is the amplitude of the considered harmonic, relative to the first,  $m_a$  is the mass of the back of the stator,  $f_n$  is the remagnetization frequency, equal to the frequency of the considered harmonic.

Induction in the back of the stator is determined based on the electromagnetic calculation of engine under nominal mode in the programming environment femm [28]. Determining the amplitude and frequency of harmonics is described above; the mass of the back of the stator is calculated using expression:

$$m_{a1} = \frac{\pi}{4} \left( (D_{a1} + 2h_{n1})^2 - D_1^2 - n_c \cdot d_c^2 \right) \cdot l_{ef1} \cdot \rho_{st}, \quad (2)$$

where  $D_{a1}$  is the outer diameter of the stator, m;  $h_{n1}$  is the height of slots in the stator, m;  $D_1$  is the inner diameter of the stator, m;  $n_c$  is the number of round ventilation ducts,  $d_c$  is the diameter of round ventilation ducts, m;  $l_{ef1}$  is the effective length of the stator package, m;  $\rho_{st}$  is the density of electrical steel,  $kg/m^3$ .

For electrical steel, we select  $\rho_{st} = 7,850 \text{ kg/m}^3$ .

Losses in the stator back are equal to:

$$P_a = 2,7 \cdot B_z^2 \cdot mag^2 \cdot m_z \left[ 0,044 \cdot f_n + 5,6 \cdot \left( \frac{f_n}{100} \right)^2 \right], \quad (3)$$

where  $B_z$  is the induction in the stator teeth, accepted to be equal to the doubled induction in the back;  $mag$  is the amplitude of the considered harmonic, relative to the first,  $m_z$  is the stator teeth mass;  $f_n$  is the remagnetization frequency equal to the frequency of the considered harmonic.

Mass of the stator teeth is equal to:

$$m_z = \frac{\pi}{4} \cdot l_{ef1} \cdot \rho_{st} \left( D_{a1}^2 - (D_{a1}^2 - 2 \cdot h_{n1})^2 - S_{n1} \cdot z \right), \quad (4)$$

where  $D_{a1}$  is the outer diameter of the stator, m;  $h_{n1}$  is the height of slots in the stator, m;  $S_{n1}$  is the stator slot area,  $m^2$ ;  $z$  is the number of stator slots;  $l_{ef1}$  is the effective length of the stator package, m;  $\rho_{st}$  is the density of electrical steel,  $kg/m^3$ .

Losses in copper from the basic frequency and harmonic components are derived from expression:

$$P_m = 3 \cdot I_f^2 \cdot k_f \cdot R_{st} \cdot t_r \cdot mag, \quad (5)$$

where  $I_f$  is the current of phase of the basic frequency, A;  $k_f$  is the Field coefficient that corresponds to the considered harmonic;  $R_{st}$  is the resistance of the cold stator winding;  $t_r$  is the temperature coefficient of copper resistance, equal to 1.58;  $mag$  is the amplitude of the considered harmonic, relative to the first.

The Field coefficients are derived from expression:

$$k_f = \frac{\phi(\xi) + \left( \frac{(m^2 - 1) \cdot \psi(\xi)}{3} - 1 \right)}{2} + 1, \quad (6)$$

where  $m$  is the number of elementary conductors in a slot,  $\phi(\xi)$ ,  $\psi(\xi)$  are the functions that take into consideration the displacement of current; they are determined according to:

$$\phi(\xi) = \xi \frac{sh2\xi + \sin 2\xi}{ch2\xi - \cos 2\xi}, \quad \psi(\xi) = 2\xi \frac{sh\xi - \sin \xi}{ch\xi + \cos \xi}, \quad (7)$$

where  $\xi$  is reduced height of the conductor, its value is equal to:

$$\xi = h_{pr} \left( \frac{b_{pr} \cdot \omega \cdot \mu_0 \cdot \lambda_m}{2 \cdot b_p} \right), \quad (8)$$

where  $h_{pr}$  is the height of the elementary conductor in the stator slot, m;  $b_{pr}$  is the width of copper in a slot, m;  $b_p$  is the width of slot in the stamp, m;  $\omega$  is the angular frequency of the considered harmonic, rad/s;  $\mu_0$  is the magnetic permeability of copper,  $Gn/m$ ;  $\lambda_m$  is the specific conductivity of copper in the winding at the expected excess in temperature  $(Ohm \cdot m)^{-1}$ .

## 6. Discussion of results of study into determining electrical losses of the traction drive

Based on the described procedure, we simulated work of the reducer-free traction drive of an electrical train based on a synchronous motor with excitation from permanent magnets with a capacity of 80 kW. We obtained dependences of losses in the traction inverter and engine on the clock frequency of space-vector PWM and motion speed.

The adequacy of the results obtained is confirmed by using the tested simulation procedures based on the software package Matlab-Simulink and the verified procedures for determining losses in the traction engines [7], as well as losses in the elements of inverters [8–10], which are widely applied in the calculation of the traction electrical equipment.

The magnitude of losses in the traction inverter lies in the range from 630 to 1,955 W. According to Fig. 13, losses in the inverter decrease with an increase in the rotations of the traction engine, which is explained by a decrease in the phase current that passes through the power keys and a snubber resistor, that is, a static component of the losses. The dynamic component of losses in the inverter increases insignificantly in the range of clock frequencies from 200 to 750 Hz; a further increase in the frequency leads to a growth

of losses, due to the increase in the number of switching in power equipment and triggering the snubber.

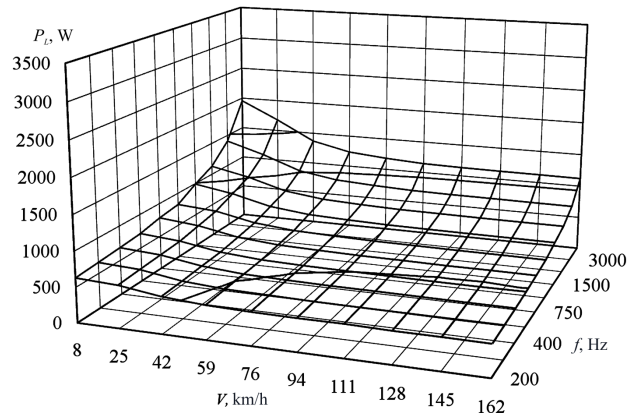


Fig. 13. Losses in the traction inverter

Losses in steel on the traction engine are shown in Fig. 14. The magnitude of losses in steel lies in the range from 70 to 1,508 W. The chart shows that the losses increase with increasing rotations of the traction engine, due to the increased frequency of the basic harmonic of phase current. A change in the clock frequency almost does not affect the magnitude of losses, due to a relatively high clock frequency of the space-vector PWM at small amplitudes of higher harmonics of the phase current.

Copper losses in the traction motor are shown in Fig. 15. The magnitude of losses is in the range from 1,100 to 3,470 W. The largest losses are observed at speeds from 0 to 40 km/h, due to a large consumed current in the traction motor. An increase in the clock frequency of a space-vector PWM of the inverter leads to a decrease in the losses in copper. This can be explained by a decrease in the amplitudes of higher harmonics of the phase current. When phase current is reduced to the rated level, the losses in copper stabilize.

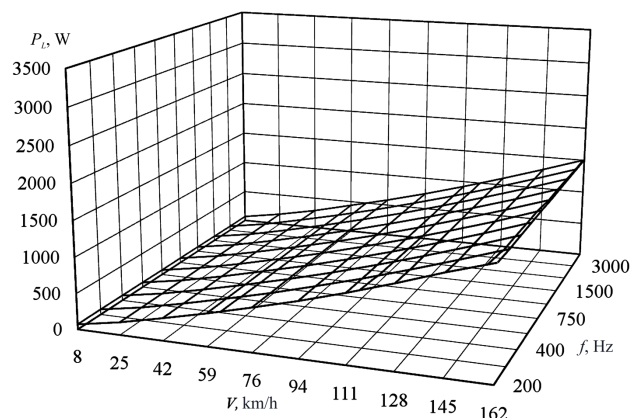


Fig. 14. Losses in steel in the traction engine

Total losses of the traction drive are shown in Fig. 16. The magnitude of losses lies within the interval from 2,270 to 5,200 W. The largest losses are observed at speeds from 0 to 25 km/h, due to work of the traction drive at starting current.

A further increase in the rotation frequency results in the stabilization of total losses at the level of 2,500...3,000 W. When speed exceeds 110 km/h, we again observe a growth of

losses, due to the increase of the component of losses in steel. The clock frequency of a space-vector PWM of the inverter slightly affects total losses, being approximately at the same level at intervals of 200...3,000 Hz. Above a clock frequency of 3,000 Hz, we observe an increase in the total losses, due to the increasing component of losses in the inverter.

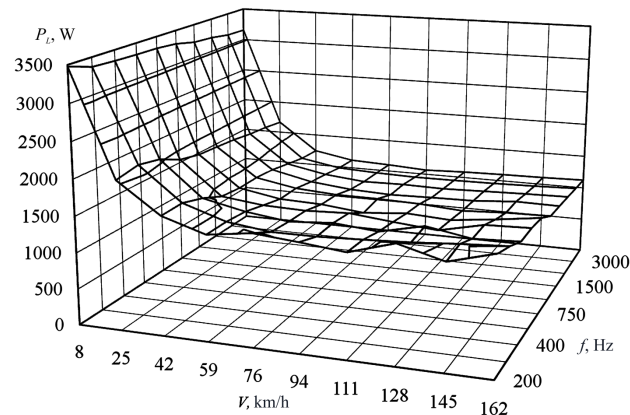


Fig. 15. Losses in steel in the traction engine

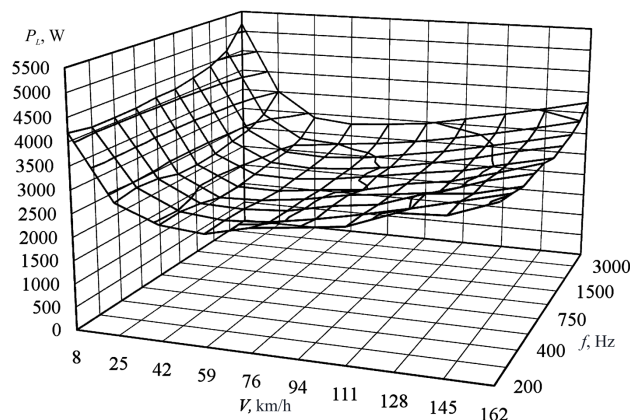


Fig. 16. Total losses in the traction drive

A further increase in the rotation frequency results in the stabilization of total losses at the level of 2,500...3,000 W. When speed exceeds 110 km/h, we again observe a growth of losses, due to the increased component of losses in steel. The clock frequency of a space-vector PWM of the inverter slightly affects total losses, being approximately at the same level at intervals of 200...3,000 Hz. Above a clock frequency of 3,000 Hz, we observe an increase in the total losses, due to the increased component of losses in the inverter.

Using the integrated simulation of the traction drive and taking into consideration the dependence of parameters of power elements in the inverter on the instantaneous values of current that passes them, we managed to account for the mutual influence of parameters of the traction engine and the inverter, as well as the effect of PWM clock frequency on losses in them.

The shortcoming of the proposed procedure is its relative complexity and large calculation time. In the further development of a given procedure, it might be possible to consider a thermal state of both the engine and the inverter, as well as calculate mechanical losses in the elements of chassis of the electric train.

The developed procedure could lay the basis to the problem on analysis of parameters of the reducer-free traction drive of electric trains based on SMPM. The analysis problem is main constituent part of the optimization complex of parameters of the traction drive for the criteria of efficiency, which were proposed by authors in [3, 4]. Its possible scope of application is control systems for the reducer-free traction drive of suburban electric trains, trams, and rail buses.

---

## 7. Conclusions

---

1. We have developed a simulation model of the drive and supplemented calculation of the components of losses in the inverter with reference dependences of parameters of the transistors on current; and applied an instantaneous value of current. Such an approach makes it possible to derive electrical losses in the inverter when using different types of IGBT-transistors, and at presence in the composition of phase currents of higher harmonics.

2. We have devised a procedure for determining losses in the engine based on the shape of phase current and parameters of the engine. The phase current, obtained from simulation modeling of the drive, decomposes into a Fourier series, thus we receive amplitudes of the primary and higher harmonic frequencies, based on which we calculate losses in steel and copper of engine.

3. It was established that for the considered drive losses in the traction inverter increase by 130...210 % when changing clock frequency from the minimum to the maximum magnitude. Losses in steel of the engine depend almost entirely on motion speed of the electric train and reach a maximum at 1,500 W at maximum speed. Losses in copper acquire a peak value of 3,500 W at the stage of initial acceleration and stabilize subsequently at the level of 1,100...1,400 W. An increase in the clock frequency from the minimum to the maximum magnitude leads to a decrease in the losses in copper by 25 %. The magnitude of total losses is described by the dependence with a complex shape. Rational clock frequency for the drive under consideration is within 200...1,000 Hz.

---

## References

1. Energy Efficiency and its contribution to energy security and the 2030 Framework for climate and energy policy. Communication from the commission to the European Parliament and the Council. Brussels, 2014. 17 p. URL: [https://ec.europa.eu/energy/sites/ener/files/documents/2014\\_eec\\_communication\\_adopted\\_0.pdf](https://ec.europa.eu/energy/sites/ener/files/documents/2014_eec_communication_adopted_0.pdf)
2. Petrenko A. N., Liubarskiy B. G., Pliugin V. E. Determination of railway rolling stock optimal movement modes // *Electrical Engineering & Electromechanics*. 2017. Issue 6. P. 27–31. doi: 10.20998/2074-272x.2017.6.04
3. Analysis of optimal operating modes of the induction traction drives for establishing a control algorithm over a semiconductor transducer / Liubarskiy B., Petrenko A., Shaïda V., Maslii A. // *Eastern-European Journal of Enterprise Technologies*. 2017. Vol. 4, Issue 8 (88). P. 65–72. doi: 10.15587/1729-4061.2017.109179
4. Optimization of thermal modes and cooling systems of the induction traction engines of trams / Liubarskiy B., Petrenko O., Iakunin D., Dubinina O. // *Eastern-European Journal of Enterprise Technologies*. 2017. Vol. 3, Issue 9 (87). P. 59–67. doi: 10.15587/1729-4061.2017.102236
5. Quality assessment of control over the traction valve-inductor drive of a hybrid diesel locomotive / Buriakovskiy S., Babaiev M., Liubarskiy B., Maslii A., Karpenko N., Pomazan D. et. al. // *Eastern-European Journal of Enterprise Technologies*. 2018. Vol. 1, Issue 2 (91). P. 68–75. doi: 10.15587/1729-4061.2018.122422
6. Cifrovoe modelirovanie tyagovogo privoda na osnove sinhronnogo tyagovogo dvigatelya s vozbuзhdeniem ot postoyannykh magnitov / Lyubarskiy B. G., Zyuzin D. Yu., Demidov A. V., Glebova T. V., Ryabov E. S. // *Visnyk Natsionalnoho tekhnichnoho universytetu "Kharkivskiy politekhnichnyi instytut"*. 2007. Issue 37. P. 111–115.
7. Proektirovanie tyagovykh elektricheskikh mashin: ucheb. pos. / M. D. Nahodkin (Ed.). izd. 2-e, pererab. i dop. Moscow: Transport, 1976. 624 p.
8. General Considerations for IGBT and Intelligent Power Modules // *Mitsubishi Application Notes*. 1998. URL: [http://www.mitsubishielectric.com/semiconductors/files/manuals/powermos3\\_0.pdf](http://www.mitsubishielectric.com/semiconductors/files/manuals/powermos3_0.pdf)
9. Zhang Y., Sobhani S., Chokhawala R. Snubber considerations for IGBT applications // *International Rectifier*. URL: <https://www.infineon.com/dgdl/tpap-5.pdf?fileId=5546d462533600a401535748b5103fe8>
10. Ivahno V. V., Zamaruev V. V., Il'ina O. V. Vybór i raschet silovykh poluprovodnikovyykh priborov poluprovodnikovogo preobrazovatelya elektricheskoy energii: ucheb. metod. pos. Kharkiv, 2014. 72 p.
11. Raschet tyagovo-energeticheskikh karakteristik teplovozov: monografiya / Golubenko A. L., Novikov V. M., Basov G. G., Tulup V. A., Tasang E. H. Lugansk: iz-vo «Noulidzh», 2011. 423 p.
12. Dvorivnevyy inverter z pokrashchenoiu formoiu vykhidnoi napruhy / Husevskiy Yu. I., Lutai S. M., Mastepan A. H., Pashynska Yu. V. // *Zbirnyk naukovykh prats Ukrainskoho derzhavnogo universytetu zaliznychnoho transportu*. 2015. Issue 153. P. 12–20.
13. A Lookup Table Based Loss Minimizing Control for FCEV Permanent Magnet Synchronous Motors / Lee J.-G., Nam K.-H., Lee S.-H., Choi S.-H., Kwon S.-W. // *Journal of Electrical Engineering and Technology*. 2009. Vol. 4, Issue 2. P. 201–210. doi: 10.5370/jeet.2009.4.2.201

14. Maximum Efficiency Control of Permanent-Magnet Synchronous Machines for Electric Vehicles / Guo Q., Zhang C., Li L., Zhang J., Wang M. // *Energy Procedia*. 2017. Vol. 105, Issue 2267–2272. doi: 10.1016/j.egypro.2017.03.650
15. Design and Implementation of a Loss Optimization Control for Electric Vehicle In-Wheel Permanent-Magnet Synchronous Motor Direct Drive System / Guo Q., Zhang C., Li L., Zhang J., Wang M. // *Energy Procedia*. 2017. Vol. 105. P. 2253–2259. doi: 10.1016/j.egypro.2017.03.644
16. A PWM for Minimum Current Harmonic Distortion in Metro Traction PMSM With Saliency Ratio and Load Angle Constrains / Zhang Z., Ge X., Tian Z., Zhang X., Tang Q., Feng X. // *IEEE Transactions on Power Electronics*. 2018. Vol. 33, Issue 5. P. 4498–4511. doi: 10.1109/tpel.2017.2723480
17. Efficiency Enhancement of Permanent-Magnet Synchronous Motor Drives by Online Loss Minimization Approaches / Cavallo C., DiTommaso A. O., Miceli R., Raciti A., Galluzzo G. R., Trapanese M. // *IEEE Transactions on Industrial Electronics*. 2005. Vol. 52, Issue 4. P. 1153–1160. doi: 10.1109/tie.2005.851595
18. Maswood A. I. A switching loss study in SPWM IGBT inverter // 2008 IEEE 2nd International Power and Energy Conference. 2008. doi: 10.1109/pecon.2008.4762548
19. System Efficiency Improvement for Electric Vehicles Adopting a Permanent Magnet Synchronous Motor Direct Drive System / Zhang C., Guo Q., Li L., Wang M., Wang T. // *Energies*. 2017. Vol. 10, Issue 12. P. 2030. doi: 10.3390/en10122030
20. Sato D., Itoh J. Total loss comparison of inverter circuit topologies with interior permanent magnet synchronous motor drive system // 2013 IEEE ECCE Asia Downunder. 2013. doi: 10.1109/ecce-asia.2013.6579149
21. An energy loss model based temperature estimation for Permanent Magnet Synchronous Motor (PMSM) / Dilshad M. R., Ashok S., Vijayan V., Pathiyil P. // 2016 2nd International Conference on Advances in Electrical, Electronics, Information, Communication and Bio-Informatics (AEEICB). 2016. doi: 10.1109/aeicb.2016.7538266
22. Power Loss Calculation and Thermal Modelling for a Three Phase Inverter Drive System / Zhou Z., Khanniche M. S., Iqbal S., Towers S. M., Mawby P. A. // *J. Electrical Systems*. 2005. Vol. 1-4. P. 33–46.
23. German-Galkin S. G. Matlab & Simulink. Proektirovanie mekhatronnyh sistem na PK. Sankr-Peterburg: KORONA-Vek, 2008. 368 p.
24. Pravila tyagovyh raschetov dlya poezdnoy raboty. Moscow: Transport, 1985. 287 p.
25. Gel'man M. V., Dudkin M. M., Preobrazhenskiy K. A. Preobrazovatel'naya tekhnika: uch. pos. Chelyabinsk: Izdatel'skiy centr YuUrGU, 2009. 425 p.
26. Kozachenko V. F. Osnovnye tendencii razvitiya vstroennykh sistem upravleniya dvigatelyami i trebovaniya k mikrokontrolle-ram // *CHIP NEWS*. 1999. Issue 1 (34). P. 2–9.
27. 2MBI400VD-120-50 IGBT module (V series) 1200V/400A/2 in one package // Fuji Electric. URL: [http://www.fujielectric-europe.com/downloads/2MBI400VD-120-50\\_1734273.PDF](http://www.fujielectric-europe.com/downloads/2MBI400VD-120-50_1734273.PDF)
28. Meeker D. Finite Element Method Magnetics Version 4.2 // 2015. URL: <http://www.femm.info/Archives/doc/manual42.pdf>